ELSEVIER

Journal of Alloys and Compounds 330–332 (2002) 743–746

Journal of ALLOYS AND COMPOUNDS

www.elsevier.com/locate/jallcom

Thermal analysis of hydrogen-induced amorphization in C15 Laves RFe_2 compounds

M. Dilixiati[a], K. Kanda[a], K. Ishikawa[a], K. Suzuki[b], K. Aoki[a,*]

[a]Kitami Institute of Technology, Kitami, Hokkaido 090-8507, Japan

[b]School of Physics, The University of New South Wales, Sydney 2052, Australia

Abstract

Structural changes of C15 Laves RFe_2 (R=Y, Ce, Sm, Gd, Tb, Dy, Ho and Er) compounds during thermal analysis in an H_2 atmosphere were investigated by scanning differential calorimetry (DSC), powder X-ray diffraction (XRD) and hydrogen analysis. Hydrogen absorption, hydrogen-induced amorphization (HIA), precipitation of RH_2 and crystallization of an amorphous phase occurred with increasing temperature for R=Y, Sm, Gd, Tb, Dy and Ho. Hydrogen absorption and HIA occurred simultaneously for R=Ce, while HIA and precipitation of ErH_2 occurred simultaneously for R=Er. The enthalpy change ΔH and the activation energy ΔE for thermal reactions of RFe_2 during heating in a hydrogen atmosphere were evaluated by DSC.

Keywords: C15 Laves phase; Hydrogen; Amorphous; Activation energy; Rare earth metal

1. Introduction

Amorphous alloys are obtained not only by rapid quenching, but also by solid state reaction such as hydrogen-induced amorphization (HIA) [1]. HIA, i.e., the transformation from a crystalline to an amorphous state by hydrogenation, has been reported to occur in intermetallic compounds having the C15, $B8_2$, $D0_{19}$ and $L1_2$ structure and containing a hydride-forming element [2,3]. Among the amorphizing compounds, HIA of C15 Laves phases RFe_2 are particularly interesting, because both crystalline and amorphous alloys form depending on the hydrogenation temperature [4,5]. However, details of thermodynamic and kinetic aspects of HIA are still uncertain. In the present work, the C15 Laves phases RFe_2 (R=a rare earth metal) are thermally analyzed in a hydrogen atmosphere. The origin of the thermal peaks and the enthalpy change and their activation energy are investigated by XRD, DSC and hydrogen analysis.

2. Experimental

RFe_2 (R=Y, Ce, Sm, Gd, Tb, Dy, Ho, Er) compounds were prepared by arc melting in an argon atmosphere. The ingots were homogenized at 973 K for 1 week in evacuated quartz tubes. Differential scanning calorimetry (DSC) was carried out at a heating rate of 0.17 K/s in H_2 of 1.0 MPa. The origin of each thermal peak was determined by heating the samples to the distinct stages in the DSC run, followed by rapid quenching to room temperature and subjecting them to the powder X-ray diffraction (XRD) analysis and the hydrogen analysis. The enthalpy change ΔH and the activation energy ΔE for each reaction in RFe_2 was calculated from the area of the DSC peak and the Kissinger's peak shift method, respectively.

3. Results and discussion

Fig. 1 shows DSC curves of RFe_2 (R=Y, Ce, Sm, Gd, Tb, Dy, Ho, Er) heated in 1.0 MPa H_2. A mark (*) shows the position of a faint exothermic peak. Three, four or five exothermic peaks are seen in these DSC curves. In the DSC curves of RFe_2 (R=Sm, Gd, Tb, Dy and Ho), four exothermic peaks, which become weak with increasing temperature, are seen. As a typical example, we focus on structural changes of $HoFe_2$ heated in an H_2 atmosphere.

Fig. 2 shows a DSC curve and the change in the hydrogen content, expressed as the atomic ratio of hydrogen to metal, H/M, of $HoFe_2$ heated in 1.0 MPa H_2.

Fig. 3 shows XRD patterns of $HoFe_2$ heated to the distinct stages of the DSC run. The XRD patterns of the original and the heated sample above the first peak (to 405 K) are indexed on the basis of C15 Laves phase, although

---

*Corresponding author.

0925-8388/02/$ – see front matter
PII: S0925-8388(01)01658-9

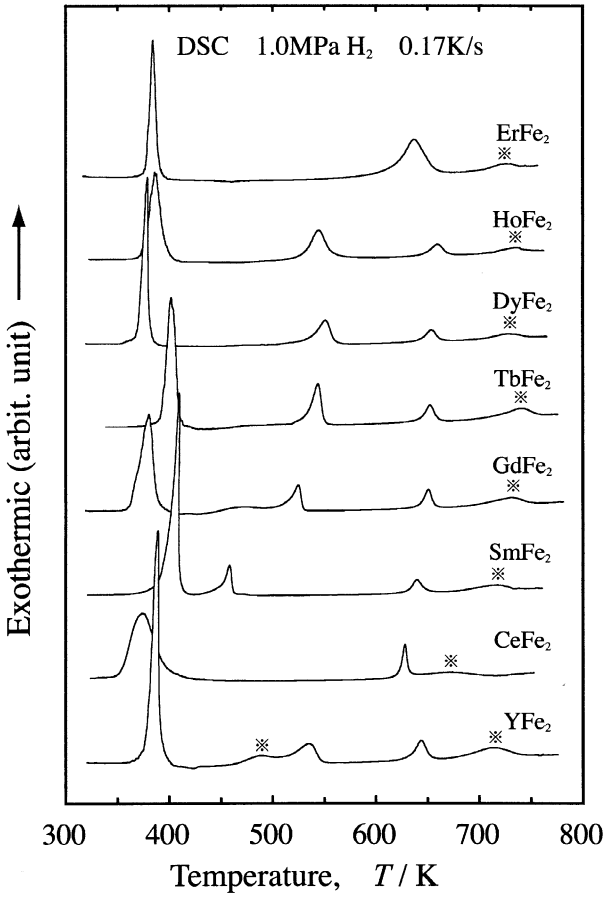

Fig. 1. DSC curves of RFe_2 (R=Y, Ce, Sm, Gd, Tb, Dy, Ho, Er) heated in 1.0 MPa H_2 at a heating rate of 0.17 K/s.

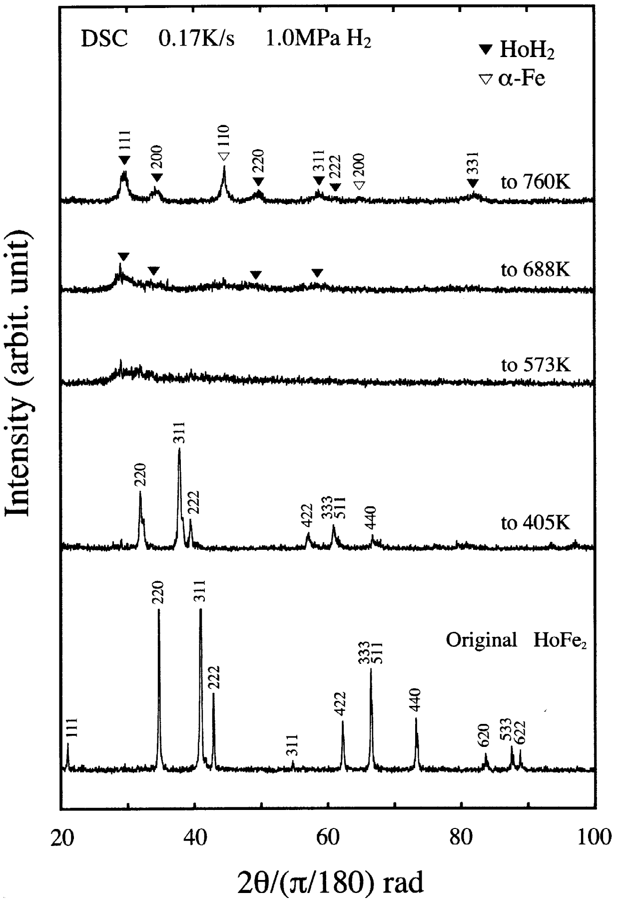

Fig. 3. XRD patterns of $HoFe_2$ heated to the distinct stages of the DSC and followed by rapid quenching to room temperature.

the Bragg peaks shift to the lower angle side by heating. The hydrogen content increases rapidly at the first peak to 1.4(H/M) and decreases gradually with increasing temperature. From XRD and the hydrogen analysis, we can see that the first exothermic peak is due to hydrogen absorption in the crystalline state and the alloy is expressed

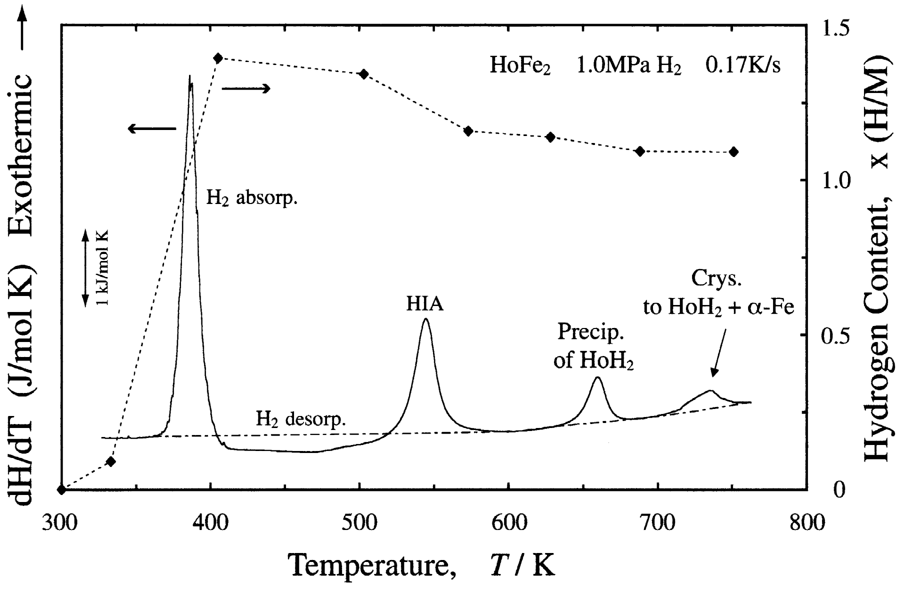

Fig. 2. A DSC curve and the change in the hydrogen content of $HoFe_2$ heated in 1.0 MPa H_2 at a heating rate of 0.17 K/s.

as crystalline c-$HoFe_2H_{1.4}$. On the contrary, the Bragg peaks disappear and are replaced by a broad peak characteristic of an amorphous phase in the XRD pattern of the sample heated above the second exothermic peak (to 573 K). A bright field image of TEM for this sample is featureless and the corresponding electron diffraction pattern shows a broad halo (not shown). Furthermore, the DSC curve of this sample shows exothermic peaks of crystallization (not shown). From these, the second exothermic peak is concluded to be due to HIA. That is, c-$HoFe_2H_{1.34}$ transforms to a-$HoFe_2H_{1.16}$ exothermally. In the XRD pattern of the sample heated above the third peak (to 688 K), new broad Bragg peaks of HoH_2 appear overlapping with the amorphous halo. The XRD pattern of the sample heated above the fourth peak (to 760 K) is indexed on the basis of HoH_2 and α-Fe.

Therefore, the third and the fourth exothermic peak is due to precipitation of HoH_2 in the amorphous phase and crystallization of the amorphous phase, respectively. The origin of each peak is written in Fig. 2. The enthalpy change, calculated from the area of DSC peak, for hydrogen absorption, HIA, precipitation of HoH_2 and crystallization is −68, −32, −9 and −14 kJ/mol, respectively. Similarly, the origin of each thermal peak for RFe_2 (for R=Y, Sm, G, Tb and Dy) was determined and the sequence of them is expressed as follows. Both hydrogenated crystalline (c-) and amorphous (a-) alloy form in these systems.

RFe_2 (for R = Y, Sm, G, Tb, Dy and Ho)

$$\text{c-RFe}_2 \underset{(\text{1st peak})}{\rightarrow} \text{c-RFe}_2\text{H}_x \underset{(\text{2nd peak})}{\rightarrow} \text{a-RFe}_2\text{H}_x \underset{(\text{3rd peak})}{\rightarrow} \text{a-R}_{1-y}\text{Fe}_2\text{H}_x + \text{RH}_2 \underset{(\text{4th peak})}{\rightarrow} \alpha\text{-Fe} + \text{RH}_2 \quad (1)$$

In the DSC curves of $CeFe_2$ and $ErFe_2$ heated in 1.0 MPa H_2, three exothermic peaks are observed. The XRD analysis indicates that hydrogen absorption and HIA occur simultaneously at the first exothermic peak of $CeFe_2$. Furthermore, the second and the third exothermic peak is due to precipitation of CeH_2 in the amorphous phase and crystallization of the remaining amorphous phase, respectively. The sequence of the thermal reactions for $CeFe_2$ with increasing temperature in H_2 is expressed as follows. Hydrogen absorbed crystalline c-$CeFe_2H_x$ is not obtained in this $CeFe_2$–H system.

$CeFe_2$

$$\text{c-CeFe}_2(\text{C15}) \underset{(\text{1st peak})}{\rightarrow} \text{a-CeFe}_2\text{H}_x \underset{(\text{2nd peak})}{\rightarrow} \text{a-Ce}_{1-y}\text{Fe}_2\text{H}_x + \text{CeH}_2 \underset{(\text{3rd peak})}{\rightarrow} \alpha\text{-Fe} + \text{CeH}_2 \quad (2)$$

On the other hand, the XRD analysis indicates that HIA and precipitation of ErH_2 occur simultaneously at the second exothermic peak of $ErFe_2$. Furthermore, the third exothermic peak is due to crystallization of the remaining amorphous phase. The sequence of the thermal reactions for $ErFe_2$ with increasing temperature in H_2 is expressed as follows. No single-phase amorphous alloy is obtained in this system.

$ErFe_2$

$$\text{c-ErFe}_2 \underset{(\text{1st peak})}{\rightarrow} \text{c-ErFe}_2\text{H}_x \underset{(\text{2nd peak})}{\rightarrow} \text{a-Er}_{1-y}\text{Fe}_2\text{H}_x + \text{ErH}_2 \underset{(\text{3rd peak})}{\rightarrow} \alpha\text{-Fe} + \text{ErH}_2 \quad (3)$$

As shown in Fig. 1, hydrogen absorption and precipitation of RH_2 occur at a nearly constant temperature. On the other hand, the peak temperature of HIA increases with increasing the atomic number of R. As a result, hydrogen absorption occurs overlapping with HIA in $CeFe_2$, while HIA occurs overlapping with precipitation of ErH_2 in $ErFe_2$.

The value of activation energy for hydrogen absorption, HIA and so on are useful to understand the HIA phenomenon in the C15 Laves compounds. The experimental value of the activation energy ΔE is determined by the Kissinger method. The method involves the application of the equation

$$\ln(C/T_p^2) = -(\Delta E/K_B T_p) + A$$

where C is the heating rate, ΔE the activation energy, T_p the peak temperature, K_B Boltzmann constant, and A is a constant.

Fig. 4 shows a schematic illustration of the enthalpy change ΔH and the activation energy ΔE for each reaction in the order of the reaction in the $HoFe_2$-H_2 system. At the first glance, we can see that the absolute value for the activation energy ΔE is larger than that of the enthalpy change ΔH for given reaction. The enthalpy change ΔH takes a smaller value in the order of hydrogen absorption, HIA, precipitation of HoH_2 and crystallization. On the other hand, the activation energy ΔE of hydrogen absorption, which is not related to the diffusion of metallic atoms, takes the smallest value. ΔE of precipitation and crystallization, which is closely related to the diffusion of the metallic atoms, takes the largest value. The reason why HIA occurs in the $HoFe_2$-H_2 system is reasonably explained on the basis of the fact that ΔE of HIA is smaller than that of precipitation of HoH_2 and crystallization.

Fig. 5 shows the activation energy ΔE_A of HIA against the reduced amorphization temperature T_a/T_m. Here, T_a and T_m is amorphization temperature and melting point of RFe_2.

HIA is considered to occur by the short-range diffusion of R and M metal. At that time, the cutting of R–M bonding is necessary for HIA. Generally, the strength of the R–M bonding is proportional to T_a/T_m. Then, it is reasonable that ΔE_A increases with increasing T_a/T_m as shown in this figure.

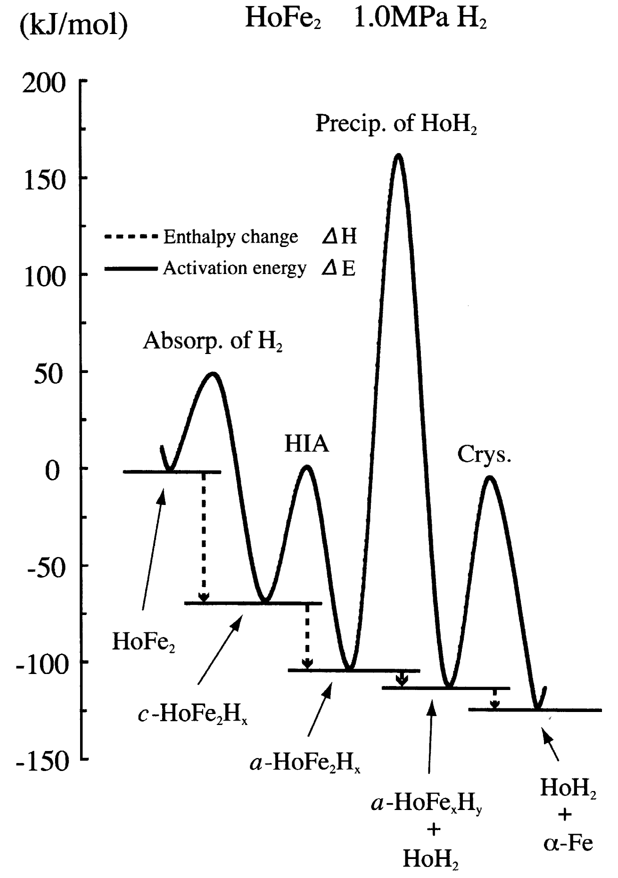

Fig. 4. A schematic illustration of enthalpy change ΔH and activation energy ΔE for each reaction in $HoFe_2$ heated in 1.0 MPa H_2 in the order of the reaction.

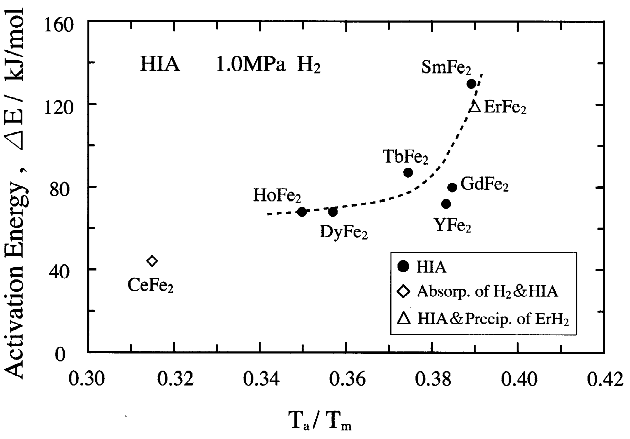

Fig. 5. Activation energy of HIA against the reduced amorphization temperature T_a/T_m.

4. Summary and conclusion

Hydrogen absorption, hydrogen-induced amorphization (HIA), precipitation of RH_2 and crystallization of the amorphous phase occur with increasing the temperature in RFe_2 for R=Y, Sm, Gd, Tb, Dy and Ho. Hydrogen absorption and HIA occur simultaneously for R=Ce, while HIA and precipitation of ErH_2 occur simultaneously for R=Er. The enthalpy change for the precipitation of HoH_2 and crystallization of the amorphous phase, which are related to the diffusion of the metallic atoms, is small, but the activation energy for them is large. The enthalpy change for hydrogen absorption is relatively large, but the activation energy of it is small. The activation energy for HIA is smaller than that for precipitation of HoH_2 and crystallization. The activation energy of HIA increases with the reduced amorphization temperature T_a/T_m.

Acknowledgements

This work was supported in part by a Grant-in-Aid for Scientific Research on Priority Areas A of ‘New Protium Function’ from the Ministry of Education, Science, Sports and Culture.

References

[1] X.L. Yeh, K. Samwer, W.L. Johnson, Appl. Phys. Lett. 42 (1983) 2482.
[2] K. Aoki, T. Yamamoto, T. Masumoto, Scripta Metall. 21 (1987) 27.
[3] K. Aoki, T. Masumoto, J. Alloys Comp. 231 (1995) 20.
[4] K. Aoki, M. Nagano, A. Yanagitani, T. Masumoto, J. Apply. Phys. 62 (1987) 3314.
[5] K. Aoki, X.-G. Li, T. Masumoto, Acta Metall. Mater. 40 (1992) 221.